INTERNATIONAL JOURNAL FOR NUMERICAL METHODS IN FLUIDS, VOL. 9, 427–452 (1989)

A CHEBYSHEV COLLOCATION METHOD FOR THE NAVIER–STOKES EQUATIONS WITH APPLICATION TO DOUBLE-DIFFUSIVE CONVECTION

U. EHRENSTEIN AND R. PEYRET

Laboratoire de Mathématiques, Université de Nice, Parc Valrose, F-06034 Nice Cedex, France

SUMMARY

A Chebyshev collocation method for solving the unsteady two-dimensional Navier–Stokes equations in vorticity–streamfunction variables is presented and discussed. The discretization in time is obtained through a class of semi-implicit finite difference schemes. Thus at each time cycle the problem reduces to a Stokes-type problem which is solved by means of the influence matrix technique leading to the solution of Helmholtz-type equations with Dirichlet boundary conditions. Theoretical results on the stability of the method are given. Then a matrix diagonalization procedure for solving the algebraic system resulting from the Chebyshev collocation approximation of the Helmholtz equation is developed and its accuracy is tested. Numerical results are given for the Stokes and the Navier–Stokes equations. Finally the method is applied to a double-diffusive convection problem concerning the stability of a fluid stratified by salinity and heated from below.

KEY WORDS Navier–Stokes equations Spectral method Chebyshev polynomials Convection

1. INTRODUCTION

During the last ten years a number of spectral methods have been proposed for the numerical solution of the Navier–Stokes equations for incompressible fluids. Most of them concern the equations in velocity–pressure variables, with various ways of handling the incompressibility condition.[1–11] However, for two-dimensional flows the formulation of the Navier–Stokes equations using vorticity ω and streamfunction ψ as dependent variables may be considered. The main advantage of this formulation is the automatic satisfaction of the incompressibility condition. Moreover, the number of equations to be solved is less than the velocity–pressure formulation. This fact, which could seem to be of minor interest, becomes really important when a large number of modes and many time cycles are needed to describe the solution. The generally recognized drawback to the vorticity–streamfunction formulation is the lack of boundary conditions for the vorticity, while there are two conditions for the streamfunction. The common way to surmount this difficulty in finite difference methods is to define ω on the boundary by the equation $\omega = -\Delta\psi$; this has been applied to spectral methods.[12, 13] Other techniques based on Green's formula and used with success in finite difference[14, 15] or finite element methods[16] have been considered for spectral approximation to Stokes-type problems.[17, 18]

In the present Chebyshev collocation method the problem of boundary conditions is solved by means of the influence matrix technique. This technique was introduced[3] to enforce the incompressibility condition at a boundary in a Chebyshev tau method for solving the primitive variable equations. Its application to the vorticity–streamfunction was considered[19] in a study of

0271–2091/89/040427–26$13.00

Received 12 October 1987
Revised 3 June 1988

axisymmetrical spherical flow, so that the boundary value problem was actually one-dimensional. Also, ordinary differential equations modelling Stokes one-dimensional problems were solved by this technique.[17] The application of the influence matrix technique to two-dimensional boundary problems is not straightforward. The main difficulty is of a mathematical nature and lies in the dimension of the spaces in which the solution must be looked for. In Reference 20 a hybrid Chebyshev tau collocation method was proposed in which the above difficulty was removed by approximating the streamfunction with more Chebyshev polynomials than the vorticity. In the pure collocation method proposed here the remedy consists in diminishing the number of boundary points on which the condition on the normal derivative of ψ is enforced. Theoretical results obtained in Reference 21 and briefly exposed below show that the resulting numerical solution for ψ is unique while the values of ω are determined in a unique way at the inner collocation points. After completion of the solution the boundary values of ω can be obtained by using the equation $\omega = -\Delta\psi$, for example.

In Section 2 the discretization in time of the Navier–Stokes equations is introduced. This is obtained through a three-parameter family of semi-implicit schemes where the diffusive term is considered in an implicit manner while the convective term is evaluated explicitly. Hence at each time step a Stokes-type problem has to be solved. The solution method of such a problem using the influence matrix technique is studied in Section 3; then the algorithm for the Navier–Stokes equations is described in Section 4. The influence matrix technique leads to the solution of Helmholtz and Poisson equations with Dirichlet conditions; hence a direct Helmholtz solver based on a matrix diagonalization procedure is developed in Section 5. Then Section 6 is devoted to numerical results for Poisson and Stokes equations. Theoretical results on the stability of the influence matrix method in an unsteady linear case are given in Section 7. Then in Section 8 numerical results for the Navier–Stokes equations are presented. Finally Section 9 is devoted to the application of the method to the solution of the equations governing double-diffusive convection flows by considering the motion of a fluid salted and heated from below.

2. THE NAVIER–STOKES EQUATIONS AND THEIR TEMPORAL DISCRETIZATION

The two-dimensional unsteady Navier–Stokes equations for an incompressible fluid are written using the vorticity ω and the streamfunction ψ as dependent variables:

$$\frac{\partial \omega}{\partial t} + \mathbf{V} \cdot \nabla \omega - \nu \Delta \omega = f, \tag{1}$$

$$\Delta \psi + \omega = 0. \tag{2}$$

In these equations ν is the kinematic viscosity and f is a given forcing term. The velocity vector $\mathbf{V} = (u, v)$ is related to the streamfunction ψ by

$$u = \partial\psi/\partial y, \qquad v = -\partial\psi/\partial x \tag{3}$$

and to the vorticity ω by

$$\omega = \partial v/\partial x - \partial u/\partial y. \tag{4}$$

Equations (1) and (2) are solved in a square domain D: $-1 < x, y < 1$, with the boundary conditions

$$\left.\begin{aligned} \psi &= g \\ \partial\psi/\partial n &= h \end{aligned}\right\} \quad \text{on} \quad \Gamma = \partial D, \tag{5}$$

where g and h are given. The function g must satisfy the total flux condition

$$\int_\Gamma (\nabla g \cdot \mathbf{t})\, ds = 0.$$

In the above equations $\mathbf{n}$ and $\mathbf{t}$ are the unit vectors respectively normal and tangent to the boundary Γ of the domain D.

The initial condition at $t=0$ is

$$\mathbf{V} = \mathbf{V}^0 = (u^0, v^0) \qquad (\nabla \cdot \mathbf{V}^0 = 0); \tag{6}$$

then

$$\omega = \omega^0 = \partial v^0/\partial x - \partial u^0/\partial y. \tag{7}$$

The time discretization makes use of a finite difference scheme. More precisely, we consider a family of schemes parametrized with ε, θ_1, θ_2 and α, so that the system (1), (2) is discretized according to

$$\frac{(1+\varepsilon)\omega^{n+1} - 2\varepsilon\omega^n - (1-\varepsilon)\omega^{n-1}}{2\Delta t} + (2\theta_1 + \theta_2)A^n + (1 - 2\theta_1 - \theta_2)A^{n-1}$$

$$-\nu[\theta_1 \Delta\omega^{n+1} + \theta_2 \Delta\omega^n + (1-\theta_1-\theta_2)\Delta\omega^{n-1}] = f^{n+\alpha}, \quad \Delta\psi^{n+1} + \omega^{n+1} = 0, \tag{8}$$

where $A = \mathbf{V}\cdot\nabla\omega$. In these equations $\omega^m \simeq \omega(x, y, m\Delta t)$ and $\psi^m \simeq \psi(x, y, m\Delta t)$. The scheme (8) is first-order accurate whatever the values of the parameters and is second-order accurate if

$$\varepsilon = 2(2\theta_1 + \theta_2 - 1) = 2\alpha. \tag{9}$$

The case $\varepsilon = 1$, $\theta_1 = 1/2$, $\theta_2 = 1/2$ corresponds to the usual Adams–Bashforth/Crank–Nicolson (AB/CN) scheme and the case $\varepsilon = 2$, $\theta_1 = 1$, $\theta_2 = 0$ gives the Adams–Bashforth/second-order backward Euler (AB/2BE) scheme introduced in Reference 20 for the Navier–Stokes equations. The stability of the above family of schemes (assuming $\theta_1 + \theta_2 = 1$) applied to the solution of the one-dimensional advection–diffusion equation with a Chebyshev collocation method has been studied in Reference 6. The stability in the case of the Stokes equations will be considered later.

At each time cycle we have to solve the following Stokes-type problem:

$$\left.\begin{aligned} \Delta\omega^{n+1} - \sigma\omega^{n+1} &= F \\ \Delta\psi^{n+1} + \omega^{n+1} &= 0 \end{aligned}\right\} \quad \text{in } D \tag{10}$$

with the boundary conditions

$$\left.\begin{aligned} \psi^{n+1} &= g^{n+1} \\ \partial\psi^{n+1}/\partial n &= h^{n+1} \end{aligned}\right\} \quad \text{on} \quad \Gamma = \partial D. \tag{11}$$

In (10) the right-hand side F contains all terms of (8) at time levels n and $n-1$ and the forcing term $f^{n+\alpha}$; finally

$$\sigma = \frac{1+\varepsilon}{2\theta_1 \nu \Delta t} > 0.$$

To start the integration ($n=0$) we assume $\omega^{-1} = \omega^0$ and $A^{-1} = A^0$ so that the scheme gives the solution at $t = 2\Delta t/3$ rather than at Δt. The solution at $t = \Delta t$ is then defined by a linear extrapolation.

In the next section we describe a direct solver for the problem (10), (11) using a Chebyshev collocation method.

3. A CHEBYSHEV COLLOCATION STOKES SOLVER

Because the problem (10), (11) has to be solved a large number of times in the course of a time-dependent solution, the Stokes solver must be efficient. First of all, this is obtained by considering a direct method avoiding any iterative procedure. Moreover, the influence matrix technique considered here reduces the problem to the solution of some number of Helmholtz and Poisson equations with Dirichlet conditions. Most of these Helmholtz-type problems are time-independent and are solved once and for all before starting integration in time.

The solution of the Helmholtz-type problems is obtained through a direct method based on a one-off matrix diagonalization process. Hence at each time cycle the solution of the Navier–Stokes equations reduces to the evaluation of matrix products, which can be performed efficiently on a vector computer. The Helmholtz solver will be described in the next section. In the present section we explain the influence matrix technique for solving (10), (11)—a technique which was presented briefly in Reference 22.

For simplicity we write (10), (11) omitting the superscript $n+1$ so that the system reads

$$\left.\begin{aligned} \Delta\omega - \sigma\omega &= F \\ \Delta\psi + \omega &= 0 \end{aligned}\right\} \quad \text{in } D, \tag{12}$$

$$\left.\begin{aligned} \psi &= g \\ \partial\psi/\partial n &= h \end{aligned}\right\} \quad \text{on } \Gamma. \tag{13}$$

We note that $\Gamma = \bigcup_{i=1}^{4} \Gamma_i$ (see Figure 1); then $g|_{\Gamma_i} = g_i$, $h|_{\Gamma_i} = h_i$, $1 \le i \le 4$. The functions g and h are assumed to satisfy the following conditions of compatibility at the corners of D.

(i) Continuity of g

$$\begin{aligned} g_1(1) &= g_2(1), & g_1(-1) &= g_4(1), \\ g_3(1) &= g_2(-1), & g_3(-1) &= g_4(-1). \end{aligned} \tag{14}$$

(ii) Compatibility of g and h

$$\begin{aligned} h_1(1) &= g_2'(1), & h_1(-1) &= g_4'(1), \\ h_2(1) &= g_1'(1), & h_2(-1) &= g_3'(1), \\ -h_3(1) &= g_2'(-1), & -h_3(-1) &= g_4'(-1), \\ -h_4(1) &= g_1'(-1), & -h_4(-1) &= g_3'(-1). \end{aligned} \tag{15}$$

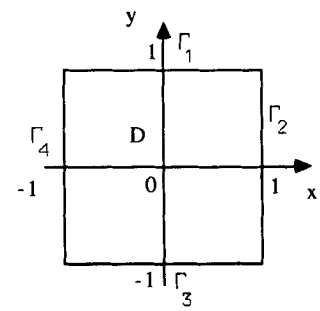

Figure 1. The domain D and its boundary $\Gamma = \bigcup_{i=1}^{4} \Gamma_i$.

(iii) Crossed derivatives

$$h_1'(1)=h_2'(1), \qquad h_1'(-1)=-h_4'(1),$$
$$h_3'(1)=-h_2'(-1), \quad h_3'(-1)=h_4'(-1). \tag{16}$$

These conditions ensure that the trace of ψ and of its derivatives on the boundary Γ are defined at the corners, and also that the equality $\partial^2\psi/\partial x\partial y=\partial^2\psi/\partial y\,\partial x$ is satisfied at the corners.

The problem (12), (13) is approximated by means of a collocation method. Let $\mathbb{P}_N$ be the set of real polynomials of degree at most equal to N and denote by

$$x_k=\cos(k\pi/N), \quad 0\le k\le N, \tag{17}$$

the Chebyshev collocation points. In terms of Chebyshev polynomial expansion, a function $\phi(x)$ approximate with the polynomial $\phi_N\in\mathbb{P}_N$ can be written as

$$\phi_N(x)=\sum_{n=0}^{N}\hat{\phi}_n T_n(x) \tag{18}$$

and the points x_k defined by (17) are the extrema of the Chebyshev polynomial $T_N(x)$. Then, there exist coefficients $d_N^{(p)}(k,i)$, $0\le i,\ k\le N$, such that the pth derivative is expressed by

$$\frac{\mathrm{d}^p\phi_N(x_k)}{\mathrm{d}x^p}=\sum_{j=0}^{N}d_N^{(p)}(k,j)\phi_N(x_j). \tag{19}$$

The expressions for $d_N^{(p)}$ for the first and second derivatives ($p=1,2$) are given in the Appendix.

Let us define now by D_c the set of collocation points in the interior of D:

$$D_c=\{x_k,\ y_l;\ 1\le k\le N,\ 1\le l\le M\},$$

where $x_k=\cos(k\pi/N)$, $y_l=\cos(l\pi/M)$; and by Γ_c the set of collocation points on the boundary. Finally, we denote by $\mathbb{P}_{N,M}$ the set of polynomials of degree at most equal to N in x and to M in y. Then the Chebyshev collocation approximation of the system (12), (13) consists in searching the $\omega_{N,M}\in\mathbb{P}_{N,M}$ and $\psi_{N,M}\in\mathbb{P}_{N,M}$ solution of *problem P*:

$$\left.\begin{aligned}\Delta\omega_{N,M}-\sigma\omega_{N,M}&=F\\ \Delta\psi_{N,M}+\omega_{N,M}&=0\end{aligned}\right\} \quad \text{in } D_c, \tag{20}$$

$$\left.\begin{aligned}\psi_{N,M}&=g\\ \partial\psi_{N,M}/\partial n&=h\end{aligned}\right\} \quad \text{on } \Gamma_c. \tag{21}$$

The various derivatives occurring in this system are expressed by formulae of the type (19), so that equations (20), (21) form an algebraic system for the values of $\omega_{N,M}$ and $\psi_{N,M}$ at the collocation points.

To solve problem P we decompose its solution $(\omega_{N,M}, \psi_{N,M})$ according to

$$\begin{aligned}\omega_{N,M}&=\tilde{\omega}_{N,M}+\bar{\omega}_{N,M}\\ \psi_{N,M}&=\tilde{\psi}_{N,M}+\bar{\psi}_{N,M},\end{aligned} \tag{22}$$

where $\tilde{\omega}_{N,M}$, $\tilde{\psi}_{N,M}$, $\bar{\omega}_{N,M}$ and $\bar{\psi}_{N,M}$ belong to $\mathbb{P}_{N,M}$. The pair $(\tilde{\omega}_{N,M}, \tilde{\psi}_{N,M})$ is the solution of *problem* $\tilde{P}$:

$$\begin{aligned}\Delta\tilde{\omega}_{N,M}-\sigma\tilde{\omega}_{N,M}&=F \quad \text{in } D_c,\\ \tilde{\omega}_{N,M}&=0 \quad \text{on } \Gamma_c,\end{aligned} \tag{23}$$

$$\begin{aligned}\Delta\tilde{\psi}_{N,M}&=-\tilde{\omega}_{N,M} \quad \text{in } D_c,\\ \tilde{\psi}_{N,M}&=g \quad \text{on } \Gamma_c.\end{aligned} \tag{24}$$

The pair $(\bar{\omega}_{N,M}, \bar{\psi}_{N,M})$ is the solution of *problem* $\bar{P}$:

$$\left.\begin{aligned} \Delta\bar{\omega}_{N,M} - \sigma\bar{\omega}_{N,M} &= 0 \\ \Delta\bar{\psi}_{N,M} + \bar{\omega}_{N,M} &= 0 \end{aligned}\right\} \quad \text{in } D_c, \tag{25a}$$

$$\left.\begin{aligned} \bar{\psi}_{N,M} &= 0 \\ \partial\bar{\psi}_{N,M}/\partial n &= h - \partial\tilde{\psi}_{N,M}/\partial n = \bar{h} \end{aligned}\right\} \quad \text{on } \Gamma_c. \tag{25b}$$

The solution of problem $\tilde{P}$ reduces to the successive solution of two elliptic equations with Dirichlet boundary conditions. The difficulty remains in the solution of problem $\bar{P}$. To solve this problem we are looking for a Dirichlet boundary condition μ for $\bar{\omega}_{N,M}$ such that if

$$\begin{aligned} \Delta\bar{\omega}_{N,M} - \sigma\bar{\omega}_{N,M} &= 0 \quad \text{in } D_c, \\ \bar{\omega}_{N,M} &= \mu \quad \text{on } \Gamma_c \end{aligned} \tag{26}$$

and

$$\begin{aligned} \Delta\bar{\psi}_{N,M} &= -\bar{\omega}_{N,M} \quad \text{in } D_c, \\ \bar{\psi}_{N,M} &= 0 \quad \text{on } \Gamma_c, \end{aligned} \tag{27}$$

then

$$\partial\bar{\psi}_{N,M}/\partial n = \bar{h} \quad \text{on } \Gamma_c. \tag{28}$$

This problem, consisting of (26)–(28), will be called *problem* P_0. We note that $\mu|_{\Gamma_i} = \mu_i$, $1 \le i \le 4$, so that $\mu_1, \mu_3 \in \mathbb{P}_N$ and $\mu_2, \mu_4 \in \mathbb{P}_M$. Furthermore, the conditions of compatibility (14) are satisfied by the μ_i; thus μ belongs to a vector space of dimension $2(N+M)$ which will be denoted by $E_{N,M}$.

In fact the problem P_0 is not well posed because we can find boundary conditions μ such that if

$$\begin{aligned} \Delta\bar{\omega}_{N,M} - \sigma\bar{\omega}_{N,M} &= 0 \quad \text{in } D_c, \\ \bar{\omega}_{N,M} &= \mu \quad \text{on } \Gamma_c, \end{aligned} \tag{29}$$

then

$$\bar{\omega}_{N,M} = 0 \quad \text{in } D_c. \tag{30}$$

The proof of this assertion is too long to be reproduced here. We only outline the main steps of the proof and refer to Reference 21 for details of the analysis.

We have to define the vector space $G_{N,M} \subset E_{N,M}$ composed of the boundary conditions μ such that (29), (30) are satisfied. For that we consider $\mu \in E_{N,M}$ and introduce the notations

$$\begin{aligned} \mu_{i,k} &= \mu_i(x_k), \quad i = 1, 3, \qquad 0 \le k \le N, \\ \mu_{i,l} &= \mu_i(y_l), \quad i = 2, 4, \qquad 0 \le l \le M. \end{aligned} \tag{31}$$

Now we consider the polynomial $\omega^*_{N,M} \in \mathbb{P}_{N,M}$ such that $\omega^*_{N,M} = 0$ on Γ_c and which coincides with the solution $\bar{\omega}_{N,M}$ of (29) at inner collocation points D_c. Therefore this polynomial $\omega^*_{N,M}$ satisfies the equations

$$\begin{aligned} \Delta\omega^*_{N,M} - \sigma\omega^*_{N,M} &= -\chi_{k,l} \quad \text{in } D_c, \\ \omega^*_{N,M} &= 0 \quad \text{on } \Gamma_c \end{aligned} \tag{32}$$

where

$$\chi_{k,l} = d^{(2)}_M(l, 0)\,\mu_{1,k} + d^{(2)}_N(k, 0)\,\mu_{2,l} + d^{(2)}_M(l, M)\,\mu_{3,k} + d^{(2)}_N(k, N)\,\mu_{4,l} \tag{33}$$

for $1 \le k \le N-1$, $1 \le l \le M-1$. The quantities $d_N^{(2)}$ and $d_M^{(2)}$ are the elements of the second-order derivation matrix defined in (19) and given in the Appendix. Note that the values of μ at the corners of the domain D do not appear in (33).

Now, if we suppose that the solution $\bar{\omega}_{N,M}$ of (29) satisfies (30), then clearly the solution $\omega^*_{N,M}$ of (32) must be the zero polynomial, which is equivalent to the condition

$$\chi_{k,l}=0, \quad 1 \le k \le N-1, \quad 1 \le l \le M-1. \tag{34}$$

Finally equations (34) are found to be satisfied if and only if

$$\begin{aligned} &\chi_{k,1}=0, \qquad \chi_{k,M-1}=0, \qquad 2 \le k \le N-2, \\ &\chi_{1,l}=0, \qquad \chi_{N-1,l}=0, \qquad 1 \le l \le M-1. \end{aligned} \tag{35}$$

Therefore equations (35) give necessary and sufficient conditions which must be satisfied by the boundary values $\mu_{i,k}$, $i=1, 3$, $1 \le k \le N-1$, and $\mu_{i,l}$, $i=2, 4$, $1 \le l \le M-1$, to ensure that $\mu \in G_{N,M}$. The algebraic system (35) consists of $2(N+M-4)$ equations for $2(N+M-2)$ unknowns; therefore its rank is $2(N+M-4)$ at most. By writing down the matrix of system (35) it is easily seen that an invertible minor of order $2(N+M-4)$ can be extracted by eliminating the four columns corresponding to $\mu_{1,1}$, $\mu_{1,N-1}$, $\mu_{3,1}$ and $\mu_{3,N-1}$, i.e. corresponding respectively to the collocation points

$$A_1=(x_1, 1), \qquad A_2=(x_{N-1}, 1), \qquad A_3=(x_1, -1), \qquad A_4=(x_{N-1}, -1). \tag{36a}$$

It follows that the system (35) defines $\mu_{i,k}$, $i=1, 3$, $2 \le k \le N-2$, and $\mu_{i,l}$, $i=2, 4$, $1 \le l \le M-1$, in terms of $\mu_{1,1}$, $\mu_{1,N-1}$, $\mu_{3,1}$ and $\mu_{3,N-1}$ in a unique way. It is likely that other choices of points leading to an invertible subsystem of (35) are possible, for example points more regularly distributed on the boundary. However, the way considered here seems to be the simplest to prove.

Thus the fact that the system (35) is of maximal rank and the above remark concerning the values of μ at the corners allow us to conclude that the dimension of $G_{N,M}$ is eight. Then, by considering the points A_i, $i=1, \ldots, 4$, defined by (36a) and also the corners

$$A_5=(1, 1), \qquad A_6=(-1, 1), \qquad A_7=(1, -1), \qquad A_8=(-1, -1), \tag{36b}$$

we define a complementary space $H_{N,M}$ of $G_{N,M}$ by

$$H_{N,M}=\{\mu \in E_{N,M} / \mu(A_i)=0, \ 1 \le i \le 8\}.$$

It follows that we have to look for a boundary condition μ belonging to $H_{N,M}$ in order to solve problem P_0, the dimension of $H_{N,M}$ being $2(N+M-4)$.

Let us now consider the boundary condition (28); when it is satisfied we have

$$\partial \bar{\psi}_{N,M}/\partial n = \bar{h}_P \quad \text{on} \quad \Gamma, \tag{37}$$

where $\bar{h}_P$ is such that $\bar{h}_{P_i}=\bar{h}_P|_{\Gamma_i}$, $1 \le i \le 4$, are the polynomials interpolating $\bar{h}|_{\Gamma_i}$ on the collocation points of Γ_i. For this to be true the $\bar{h}_{P_i}$ have to satisfy both conditions (15) where $g_i=0$ and conditions (16). These conditions will be satisfied up to the accuracy of the Chebyshev polynomial approximation to the boundary conditions g and h of (21). Therefore the conditions (15) imply that

$$\bar{h}_{P_i}(\pm 1)=0, \quad 1 \le i \le 4,$$

and by the further conditions (16) it can be seen that $\bar{h}_P$ is entirely determined by its values at the points of $\Gamma_c'=\Gamma_c-\{A_1, \ldots, A_8\}$, where A_i, $1 \le i \le 8$, are the points defined in (36). Thus $\bar{h}_P$ belongs to a vector space of dimension $2(N+M-4)$.

If we suppose now that the only solutions of problem P_0 with

$$\partial\bar{\psi}_{N,M}/\partial n=0 \quad \text{on} \quad \Gamma$$

are such that $\mu\in G_{N,M}$, then according to the above considerations the problem P_0 admits a unique solution $\mu\in H_{N,M}$. Furthermore, by the definition of the vector space $G_{N,M}$ we see that the solution of problem P_0 is unique for $\bar{\psi}_{N,M}$ but only the values of $\bar{\omega}_{N,M}$ in D_c are determined in a unique manner.

The method of solution of problem P_0 is based upon the technique of superposition of elementary solutions. More precisely, if η_j, $1\le j\le J=2(N+M-4)$, represent the points of Γ_c', we define the characteristic function $\rho_j\in E_{N,M}$ by $\rho_j(\eta_j)=1$ and $\rho_j=0$ on all other points of Γ_c. Then we define the family (ω_j,ψ_j), $1\le j\le J$, where ω_j, $\psi_j\in\mathbb{P}_{N,M}$, as the solutions of

$$\begin{aligned}\Delta\omega_j-\sigma\omega_j&=0 \quad \text{in } D_c,\\ \omega_j&=\rho_j \quad \text{on } \Gamma_c,\end{aligned} \tag{38}$$

$$\begin{aligned}\Delta\psi_j&=-\omega_j \quad \text{in } D_c,\\ \psi_j&=0 \quad \text{on } \Gamma_c,\end{aligned} \tag{39}$$

and the solution μ, $\bar{\omega}_{N,M}$, $\bar{\psi}_{N,M}$ of problem P_0 is constructed as

$$\mu=\sum_{j=1}^{J}\lambda_j\rho_j, \tag{40}$$

$$\begin{pmatrix}\bar{\omega}_{N,M}\\ \bar{\psi}_{N,M}\end{pmatrix}=\sum_{j=1}^{J}\lambda_j\begin{pmatrix}\omega_j\\ \psi_j\end{pmatrix}. \tag{41}$$

The coefficients λ_j, $1\le j\le J$, are determined so that the Neumann boundary condition (37) is satisfied on points η_j of Γ_c'. By doing that we get the algebraic system

$$\mathbf{M}\boldsymbol{\Lambda}=\bar{\mathbf{H}},$$

where $\boldsymbol{\Lambda}=(\lambda_1,\ldots,\lambda_J)^T$, $\bar{\mathbf{H}}=(\bar{h}_P(\eta_1),\ldots,\bar{h}_P(\eta_J))^T$ and the influence matrix $\mathbf{M}=[m_{i,j}]$, $1\le i,j\le J$, is defined by

$$m_{i,j}=\frac{\partial\psi_j}{\partial n}(\eta_i), \quad \eta_i\in\Gamma_c'.$$

When $\boldsymbol{\Lambda}$ is known the solution $\omega_{N,M}$, $\psi_{N,M}$ is determined by (22) and (41). As already pointed out, the method gives $\omega_{N,M}$ in a unique way in D_c only. The values of $\omega_{N,M}$ on Γ_c given by the algorithm would be correct if the exact solution ω was zero at points A_i, $1\le i\le 8$. It is obvious that this is not true in general and the values of $\omega_{N,M}$ on Γ_c (if needed) can be defined by the equation $\omega_{N,M}=-\Delta\psi_{N,M}$ written on Γ_c.

In the tau collocation influence matrix technique introduced in Reference 20 the difficulty associated with the non-uniqueness of μ was surmounted by approximating ω and ψ with polynomials belonging to $\mathbb{P}_{N,M}$ and $\mathbb{P}_{N+2,M+2}$ respectively.

4. ALGORITHM FOR THE NAVIER–STOKES EQUATIONS

As explained in Section 2, the solution of the unsteady Navier–Stokes equations is reduced to the solution of a Stokes-type problem at each time step. This problem is solved by the influence matrix

technique described in the previous section. The matrix of influence $\mathbf{M}$ being time-independent, it can be constructed and inverted once and for all before starting the time integration. Then at each time step we solve the problem $\tilde{\mathbf{P}}$ which defines $(\bar{\omega}_{N,M}, \bar{\psi}_{N,M})$, we construct $\bar{\mathbf{H}}$ and $\mathbf{\Lambda}$ is determined by

$$\mathbf{\Lambda} = \mathbf{M}^{-1}\bar{\mathbf{H}}.$$

At this point several ways of calculating $(\omega_{N,M}, \psi_{N,M})$ are possible according to the computer facilities available (memory, vectorization or parallelization). For example:

1. The solution $(\omega_{N,M}, \psi_{N,M})$ is calculated from (22) with $(\bar{\omega}_{N,M}, \bar{\psi}_{N,M})$ obtained through the summation (41).
2. The summation can be reduced by calculating $\bar{\psi}_{N,M}$ from (41) and $\bar{\omega}_{N,M}$ by the equation
$$\bar{\omega}_{N,M} = -\Delta\bar{\psi}_{N,M}.$$
3. The summation can be avoided completely by calculating $(\omega_{N,M}, \psi_{N,M})$ as the solution of the two Dirichlet problems
$$\begin{aligned} \Delta\omega_{N,M} - \sigma\omega_{N,M} &= F && \text{in } D_c, \\ \omega_{N,M}(\eta_j) &= \lambda_j, && \eta_j \in \Gamma_c', \quad 1 \le j \le J, \\ \omega_{N,M} &= 0 && \text{on } \Gamma_c - \Gamma_c' \end{aligned}$$
and
$$\begin{aligned} \Delta\psi_{N,M} &= -\omega_{N,M} && \text{in } D_c, \\ \psi_{N,M} &= 0 && \text{on } \Gamma_c. \end{aligned}$$

This third technique is used in the calculations reported below.

Therefore the solution of the Navier–Stokes equations is reduced to: (1) the evaluation of the right-hand side F of equation (23); (2) the solution of Helmholtz-type equations with Dirichlet boundary conditions. The global efficiency of the method depends strongly on the manner in which these two operations are performed.

The evaluation of the non-linear convective term $\mathbf{V}\cdot\nabla\omega$ in F can be done either by the usual pseudospectral technique (products in the physical space, differentiations in the spectral space, link of both spaces by a FFT algorithm) or by matrix products in the physical plane using (19) for derivatives. This second technique has been employed here using an efficient vectorized subroutine for matrix products (MXM of SCILIB). For a moderate number of Chebyshev polynomials this technique is competitive with the pseudospectral technique.

The Helmholtz equations are solved by means of a fast direct solver which is very efficient when a large number of problems have to be solved like here. This solver is described in the following section.

5. A DIRECT HELMHOLTZ SOLVER

The Helmholtz solver is an adaptation to the case of the collocation Chebyshev approximation of the matrix diagonalization procedure introduced in Reference 23 for the tau Chebyshev approximation. To illustrate the technique we consider the Dirichlet problem

$$\Delta u - \sigma u = f \quad \text{in } D, \tag{42}$$

$$u = g \quad \text{on } \Gamma, \tag{43}$$

where $\sigma = \text{const} \geq 0$, f and g are given. Let $u_{N,M}$ be the polynomial approximation to the solution of (42), (43) and (x_k, y_l), $0 \leq k \leq N$, $0 \leq l \leq M$, be the Chebyshev collocation points. The derivatives in (42) are expressed in terms of $u_{N,M}(x_k, y_l)$ by formulae of the type (19). Then the boundary values $u_{N,M}(x_k, \pm 1)$, $1 \leq k \leq N-1$, and $u_{N,M}(\pm 1, y_l)$, $0 \leq l \leq M$, are eliminated thanks to the boundary condition (43). Hence the matrix $\mathbf{U}_{N,M} = [u_{N,M}(x_k, y_l)]$, $1 \leq k \leq N-1$, $1 \leq l \leq M-1$, is the solution of

$$\mathbf{D}_x^{(2)} \mathbf{U}_{N,M} + \mathbf{U}_{N,M} \mathbf{D}_y^{(2)\mathrm{T}} - \sigma \mathbf{U}_{N,M} = \mathscr{F}, \tag{44}$$

where $\mathbf{D}_x^{(2)}$ and $\mathbf{D}_y^{(2)}$ are the matrices

$$\mathbf{D}_x^{(2)} = [d_N^{(2)}(k, l)], \quad 1 \leq k, l \leq N-1,$$

$$\mathbf{D}_y^{(2)} = [d_M^{(2)}(k, l)], \quad 1 \leq k, l \leq M-1,$$

with $d_N^{(2)}$ and $d_M^{(2)}$ the coefficients appearing in equation (19) and given in the Appendix. Finally $\mathscr{F}$ is the matrix

$$\mathscr{F} = [F(x_k, y_l)], \quad 1 \leq k \leq N-1, \quad 1 \leq l \leq M-1,$$

with

$$F(x_k, y_l) = f(x_k, y_l) - d_M^{(2)}(l, 0) g_1(x_k) - d_M^{(2)}(l, M) g_3(x_k) - d_N^{(2)}(k, 0) g_2(y_l) - d_N^{(2)}(k, N) g_4(y_l),$$

where we have introduced, as in Section 3, $g_i = g|_{\Gamma_i}$ and $\Gamma = \bigcup_{i=1}^{4} \Gamma_i$ (see Figure 1). As proven in Reference 24, the eigenvalues of each of the matrices $\mathbf{D}_x^{(2)}$ and $\mathbf{D}_y^{(2)}$ are real, distinct and negative. These matrices can be diagonalized; therefore

$$\mathbf{S}_x^{-1} \mathbf{D}_x^{(2)} \mathbf{S}_x = \text{diag}(\lambda_{x,1}, \ldots, \lambda_{x,N-1}) = \mathbf{\Lambda}_x,$$

where $\lambda_{x,1}, \ldots, \lambda_{x,N-1}$ are the eigenvalues of $\mathbf{D}_x^{(2)}$ and $\mathbf{S}_x$ is the matrix of the associated eigenvectors. By multiplying (44) on the left by $\mathbf{S}_x^{-1}$ we obtain

$$\mathbf{\Lambda}_x \hat{\mathbf{U}}_{N,M} + \hat{\mathbf{U}}_{N,M} \mathbf{D}_y^{(2)\mathrm{T}} - \sigma \hat{\mathbf{U}}_{N,M} = \hat{\mathscr{F}}, \tag{45}$$

where

$$\hat{\mathbf{U}}_{N,M} = \mathbf{S}_x^{-1} \hat{\mathbf{U}}_{N,M} = [\hat{u}_{k,l}], \qquad \hat{\mathscr{F}} = \mathbf{S}_x^{-1} \mathscr{F} = [\hat{F}_{k,l}].$$

Therefore the solution of the system (44) reduces to the solution of $N-1$ 'one-dimensional' systems:

$$[\mathbf{D}_y^{(2)} + (\lambda_{x,k} - \sigma)\mathbf{I}] \hat{\mathbf{U}}_k = \hat{\mathscr{F}}_k, \quad 1 \leq k \leq N-1, \tag{46}$$

where

$$\hat{\mathbf{U}}_k = (\hat{u}_{k,1}, \ldots, \hat{u}_{k,M-1})^{\mathrm{T}}, \qquad \hat{\mathscr{F}}_k = (\hat{F}_{k,1}, \ldots, \hat{F}_{k,M-1})^{\mathrm{T}}.$$

The solution of (46) can be obtained by direct inversion without or with preconditioning to prevent numerical inaccuracies due to the ill conditioning of the matrix $\mathbf{D}_y^{(2)} + (\lambda_{x,k} - \sigma)\mathbf{I}$.

Following Reference 25, we may also perform a second diagonalization in the y-direction. In this case $\mathbf{D}_y^{(2)}$ is diagonalized as

$$\mathbf{S}_y^{-1} \mathbf{D}_y^{(2)} \mathbf{S}_y = \text{diag}(\lambda_{y,1}, \ldots, \lambda_{y,M-1}) = \mathbf{\Lambda}_y$$

and equation (45) becomes, after multiplication on the right by $(\mathbf{S}_y^{-1})^{\mathrm{T}}$,

$$\mathbf{\Lambda}_x \hat{\mathbf{U}}_{N,M} (\mathbf{S}_y^{-1})^{\mathrm{T}} + \hat{\mathbf{U}}_{N,M} (\mathbf{S}_y^{-1})^{\mathrm{T}} \mathbf{\Lambda}_y - \sigma \hat{\mathbf{U}}_{N,M} (\mathbf{S}_y^{-1})^{\mathrm{T}} = \hat{\mathscr{F}} (\mathbf{S}_y^{-1})^{\mathrm{T}}, \tag{47}$$

where we have taken into account $\mathbf{S}_y^{\mathrm{T}}\mathbf{D}_y^{(2)\mathrm{T}}(\mathbf{S}_y^{-1})^{\mathrm{T}}=\mathbf{\Lambda}_y$. Equation (47) can be rewritten as

$$(\lambda_{x,k}+\lambda_{y,l}-\sigma)\tilde{u}_{k,l}=\tilde{F}_{k,l}, \quad 1\le k\le N-1, \quad 1\le l\le M-1, \tag{48}$$

where $\tilde{u}_{k,l}$ and $\tilde{F}_{k,l}$ are the entries of matrices $\hat{\mathbf{U}}_{N,M}(\mathbf{S}_y^{-1})^{\mathrm{T}}$ and $\hat{\mathscr{F}}(\mathbf{S}_y^{-1})^{\mathrm{T}}$ respectively. Equations (48) give the solution $\tilde{u}_{k,l}$ from which the solution $u_{N,M}(x_k, y_l)$ can be obtained.

Numerical results from the various techniques described above will be presented in Section 6.

It must be remembered that algorithms of diagonalization are efficient when a large number of Helmholtz problems (42), (43) have to be solved in the course of an unsteady calculation. In this case the calculation of eigenvalues, eigenvectors and the inversion of the matrices can be done once and for all before starting the time integration.

Finally we point out that the method can be applied to any type of boundary conditions,[21] the technique being to eliminate the boundary values thanks to the boundary conditions, as done in the Dirichlet case.

6. NUMERICAL RESULTS FOR POISSON AND STOKES EQUATIONS

The algorithms described in the previous sections have been applied to test cases in order to evaluate their properties.

6.1. Poisson equation

We consider the Poisson equation with Dirichlet conditions

$$\Delta u=f \quad \text{in } D\text{: } -1<x, y<1, \tag{49a}$$

$$u=0 \quad \text{on } \Gamma=\partial D, \tag{49b}$$

with the exact solution

$$u_{\mathrm{ex}}=\sin(4\pi x)\sin(4\pi y) \tag{50}$$

which defines the forcing term f in (49a). The solution of problem (49) is obtained by the collocation Chebyshev method using the matrix diagonalization procedure described in Section 5. Table I shows the maximum error on collocation points given by the various techniques of Section 5. The degree of the polynomials is the same in both directions, that is $N=M$. The calculations were done with a CRAY 1S computer (providing 14 accurate digits).

(i) E_1 is the error obtained when the matrices $\mathbf{L}_k=\mathbf{D}_y^{(2)}+(\lambda_{x,k}-\sigma)\mathbf{I}$, $1\le k\le N-1$, in (46) are inverted by using the subroutines SGECO/SGEDI of SCILIB. The important loss of accuracy between $N=32$ and $N=64$ is mainly due to the ill conditioning of the matrices $\mathbf{L}_k$.

Table I. Errors for the Poisson equation

$N=M$	E_1	E_2	E_3	E_4	E_5
12	8·83 E-2	8·83 E-2	8·83 E-2	8·83 E-2	2·70 E-1
16	5·25 E-3	5·25 E-3	5·25 E-3	5·25 E-3	3·33 E-2
20	7·52 E-5	7·52 E-5	7·52 E-5	7·52 E-5	8·19 E-4
24	4·05 E-7	4·05 E-7	4·05 E-7	4·05 E-7	6·89 E-6
32	7·65 E-12	2·84 E-12	2·86 E-12	2·87 E-12	4·95 E-11
40	1·38 E-11	1·23 E-12	1·26 E-12	1·47 E-12	6·06 E-12
48	1·54 E-11	2·31 E-12	2·21 E-12	3·63 E-12	8·79 E-12
64	2·07 E-11	3·68 E-12	3·78 E-12	3·90 E-12	2·93 E-11

(ii) E_2 is the error obtained by preconditioning $\mathbf{L}_k$ before inversion. Let $\mathbf{A}_k$ be the matrix associated with the three-point centred finite difference approximation of $\partial^2/\partial y^2 + (\lambda_{x,k} - \sigma)1$ using the Chebyshev points. This tridiagonal matrix $\mathbf{A}_k$ serves as a preconditioning matrix for $\mathbf{L}_k$, so that the matrices to be inverted are now $\mathbf{B}_k = \mathbf{A}_k^{-1}\mathbf{L}_k$, $1 \leq k \leq N-1$, which are well conditioned.[26] The inversion is performed again with SGECO/SGEDI. The gain in accuracy for high values of N is clearly seen.

(iii) However, equivalent results (error E_3) are obtained without preconditioning but by inverting $\mathbf{L}_k$ with a more elaborate inversion subroutine (LINV2F of IMSL).

(iv) The error E_4 given by the full diagonalization technique (equation (48)) is comparable to errors E_2 and E_3.

(v) The error E_5 concerns the case of the tau Chebyshev approximation of (49) associated with the partial diagonalization algorithm[12,25] inspired by Reference 23. The solution of the resulting one-dimensional problems reduces to the inversion of quasi-tridiagonal matrices (for odd and even modes).

We may observe that the collocation method is slightly more accurate than the tau method provided the problem of ill conditioning of collocation matrices is correctly handled. The loss of accuracy observed when N is large can be attributed to round-off errors associated with the various numerical processes: calculation of eigenvalues and eigenvectors, inversion of matrices, etc. In this respect it must be pointed out that the conditioning of the eigenvector matrix $\mathbf{S}_x$ (or $\mathbf{S}_y$) is comparable and even better in the collocation method. For $24 \leq N \leq 64$ we found the condition number

$$K(\mathbf{S}_x) = \sqrt{(\lambda_{\max}/\lambda_{\min})} \simeq 0{\cdot}80\, N^{0{\cdot}25},$$

where $\lambda_{\max}$ and $\lambda_{\min}$ are respectively the largest and smallest eigenvalues of $\mathbf{S}_x\mathbf{S}_x^{\mathrm{T}}$. For $N = 32$ this gives $K \simeq 1{\cdot}90$ which must be compared with $K \simeq 4{\cdot}24$ obtained in the tau method of Reference 23.

6.2. *Stokes equations*

The collocation Chebyshev influence matrix technique described in Section 4 has been used to solve the Stokes problem

$$\left.\begin{aligned} \Delta\omega &= f \\ \Delta\psi + \omega &= 0 \end{aligned}\right\} \quad \text{in } D\text{: } -1 < x, y < 1, \tag{51}$$

$$\left.\begin{aligned} \psi &= 0 \\ \partial\psi/\partial n &= h \end{aligned}\right\} \quad \text{on } \Gamma = \partial D, \tag{52}$$

with the exact solution

$$\psi_{\mathrm{ex}} = \sin(4\pi x)\sin(4\pi y), \qquad \omega_{\mathrm{ex}} = 32\pi^2\psi_{\mathrm{ex}} \tag{53}$$

which defines f and h. The Poisson equations occurring in the influence matrix method are solved by the algorithm described in (ii) of Section 6.1 (partial matrix diagonalization, inversion after finite difference preconditioning). The results are reported in Table II: E_∞^ϕ with $\phi = \{\psi, \omega\}$ is the maximum error on all collocation points normalized with the maximum norm $\|\phi\|_\infty$; $E_{\infty 1}^\omega$ is the analogous error on inner collocation points; E_2^ϕ is the discrete L_2 error normalized by the L_2 norm of ϕ; $\hat{E}_\infty^\phi$ is the maximum error, normalized with $\|\phi\|_\infty$, of the Chebyshev coefficients $\hat{\phi}_n$ (equation (18)) with respect to the coefficients of the exact solution. Both these spectra being calculated by means of a FFT algorithm using the same number of collocation

Table II. Errors for the Stokes equations

$N=M$	E_∞^ψ	E_2^ψ	E_∞^ω	$E_{\infty 1}^\omega$	E_2^ω	$\hat{E}_\infty^\psi$	$\hat{E}_\infty^\omega$
16	1·32E−2	1·40E−2	2·63E−1	2·96E−2	2·88E−1	3·92E−3	8·20E−2
24	3·75E−6	3·10E−6	1·69E−4	7·35E−6	1·67E−4	9·47E−7	4·69E−5
32	3·55E−11	2·81E−11	2·85E−9	7·16E−11	2·72E−9	8·57E−12	7·26E−10
40	2·95E−12	1·19E−12	3·36E−11	3·61E−12	1·65E−11	3·14E−13	5·00E−12
48	3·45E−12	1·77E−12	5·57E−11	4·24E−12	4·09E−11	5·20E−13	1·17E−11
64	4·68E−12	2·55E−12	2·56E−10	1·58E−11	1·79E−11	7·99E−13	5·92E−11

points, the quantity $\hat{E}_\infty^\phi$ measures the accuracy of the numerical algorithm but not the accuracy of the polynomial approximation.

The comparison of E_∞^ω and $E_{\infty 1}^\omega$ in Table II shows that the error is maximum on the boundary itself. We recall that the influence matrix method gives the values of ω at inner collocation points only. Here the boundary values of ω have been determined by using $\omega = -\Delta\psi$ on the boundary.

We have also compared the results given by the present collocation method with those obtained through the tau collocation influence matrix technique proposed in Reference 20. The results are comparable, with again some advantage to the pure collocation approximation. It was observed that the influence matrix is better conditioned in the present method. For the Stokes-type problem (12), (13), we numerically found the condition number

$$K(\mathbf{M}) \simeq a(\sigma) N^{1\cdot 96}$$

with $a(0)=0\cdot 46$ and $a(1000)=0\cdot 03$.

The high accuracy of the method was also made evident in Reference 22 through the calculation of the secondary eddies appearing in the Stokes flow in a corner.

7. STABILITY OF THE INFLUENCE MATRIX TECHNIQUE

When the influence matrix technique is employed for solving the Stokes-type problem at each time cycle of the unsteady solution of the Navier–Stokes equation an important question concerns the stability of the time discretization scheme. Results on the stability of the schemes of type (8) applied to the solution of the one-dimensional advection–diffusion equation have been presented in Reference 6. However, these results cannot be applied directly to the present problem because of the presence of the ψ-equation and mainly because of the boundary conditions and the manner of their implementation through the influence matrix method.

In this section some theoretical results on the stability of the method are given in the special case where (1) convective terms in (1) are neglected (the unsteady Stokes approximation) and (2) the solution is assumed to be 2π-periodic in the y-direction. Then, by expanding the solution $\omega(x, y, t)$, $\psi(x, y, t)$ in Fourier series in the y-direction, we obtain for each Fourier component $\omega_\kappa(x, t)$, $\psi_\kappa(x, t)$ corresponding to the frequency κ the following problem:

$$\left.\begin{aligned} &\partial\omega_\kappa/\partial t - \nu(\partial^2\omega_\kappa/\partial x^2 - \kappa^2\omega_\kappa) = 0 \\ &(\partial^2\psi_\kappa/\partial x^2) - \kappa^2\psi_\kappa + \omega_\kappa = 0 \end{aligned}\right\} \quad -1 < x < 1, \tag{54}$$

$$\psi_\kappa(\pm 1, t) = 0, \qquad \partial\psi_\kappa/\partial x(\pm 1, t) = 0, \tag{55}$$

$$\omega_\kappa(x, 0) = \omega_\kappa^0(x), \tag{56}$$

where we have assumed $f=g=h=0$. This assumption is not restrictive for a stability analysis.

The above system is discretized with respect to time according to the scheme (8), so that $\omega_\kappa^{n+1}(x)$, $\psi_\kappa^{n+1}(x)$ is the solution of a one-dimensional Stokes-type problem analogous to (10), (11). This problem is solved by using the collocation Chebyshev influence matrix method developed in Section 3. We denote by $(\omega_N^{n+1}, \psi_N^{n+1})$ the polynomial approximation to the solution $(\omega_\kappa^{n+1}, \psi_\kappa^{n+1})$. The method involves the following decomposition:

$$\begin{pmatrix} \omega_N^{n+1} \\ \psi_N^{n+1} \end{pmatrix} = \begin{pmatrix} \tilde{\omega}_N^{n+1} \\ \tilde{\psi}_N^{n+1} \end{pmatrix} + \sum_{j=1}^{2} \lambda_j^{n+1} \begin{pmatrix} \omega_{jN} \\ \psi_{jN} \end{pmatrix}. \tag{57}$$

The pair $(\tilde{\omega}_N^{n+1}, \tilde{\psi}_N^{n+1})$ is the solution of problem $\tilde{\mathrm{P}}$ analogous to (23), (24). The pairs (ω_{jN}, ψ_{jN}), $j=1, 2$, are analogous to (ω_j, ψ_j) defined in (38), (39) with $\omega_{1N}(-1)=1$, $\omega_{1N}(1)=0$, $\omega_{2N}(-1)=0$, $\omega_{2N}(1)=1$. Finally the coefficients λ_j^{n+1}, $j=1, 2$, are determined so that the second boundary condition (55) is satisfied. The values $\tilde{\psi}_N^m(x_k)$, $x_k=\cos(k\pi/N)$, $0\le k\le N$, can be expressed in terms of the values $\tilde{\omega}_N^m(x_k)$ and it is the same for the coefficients λ_j^m, $j=1, 2$. Therefore the study of the stability of the scheme can be reduced to the study of

$$\tilde{\mathbf{\Omega}}^{n+1} = \mathbf{A}\tilde{\mathbf{\Omega}}^n + \mathbf{B}\tilde{\mathbf{\Omega}}^{n-1}, \tag{58}$$

where $\tilde{\mathbf{\Omega}}^m = [\tilde{\omega}_N^m(x_1), \ldots, \tilde{\omega}_N^m(x_{N-1})]^{\mathrm{T}}$, $\mathbf{A}$ and $\mathbf{B}$ are two matrices which depend on $\nu\Delta t$, N, κ^2 and on the parameters of the scheme ε, θ_1 and θ_2.

By introducing $\tilde{\mathbf{\Phi}}^n = \tilde{\mathbf{\Omega}}^{n-1}$, equation (58) becomes

$$\begin{pmatrix} \tilde{\mathbf{\Omega}}^{n+1} \\ \tilde{\mathbf{\Phi}}^{n+1} \end{pmatrix} = \mathbf{E} \begin{pmatrix} \tilde{\mathbf{\Omega}}^n \\ \tilde{\mathbf{\Phi}}^n \end{pmatrix}, \tag{59}$$

where

$$\mathbf{E} = \begin{pmatrix} \mathbf{A} & \mathbf{B} \\ \mathbf{I} & \mathbf{0} \end{pmatrix}. \tag{60}$$

A necessary condition for stability is that $\rho(\mathbf{E})\le 1$ where $\rho(\mathbf{E})$ is the spectral radius of $\mathbf{E}$. For some special schemes of the family (8) the following results are proven in Reference 21. For the schemes $0<\theta_1\le 1$, $\theta_2=1-\theta_1$ and either $\varepsilon=1$ or $\varepsilon=2\theta_1$ the matrix $\mathbf{E}$ has at least one eigenvalue whose absolute value is $(1-\theta_1)/\theta_1$. Also, for the schemes $0<\theta_1\le 1$, $\theta_2=0$ and $\varepsilon=2(2\theta_1-1)$, $\mathbf{E}$ has eigenvalues equal to $\pm i\sqrt{[(1-\theta_1)/\theta_1]}$. Hence the condition $\rho(\mathbf{E})\le 1$ necessitates $\theta_1\ge 1/2$. In fact for all these special schemes it can be proven that

(i) $\rho(\mathbf{E})>1$ if $0<\theta_1<1/2$,
(ii) $\rho(\mathbf{E})=1$ if $\theta_1=1/2$,
(iii) $\rho(\mathbf{E})<1$ if $1/2<\theta_1\le 1$.

The result (i) is remarkable: it shows that schemes for which $\theta_1<1/2$ are unconditionally unstable, while the same schemes applied to the diffusion equation alone are conditionally stable.[6] The result (ii) shows that the stability of the usual Crank–Nicolson scheme ($\varepsilon=1$, $\theta_1=\theta_2=1/2$) can be defined as marginal. Finally schemes belonging to case (iii) seem to have the best property of stability. In particular the second-order Euler backward scheme ($\varepsilon=2$, $\theta_1=1$, $\theta_2=0$) has been used with success[20,27] in the solution of the Navier–Stokes equations. Its application to the calculation of a time-periodic flow (Section 9) showing no damping of the oscillations is a guarantee that this scheme is not too dissipative, even if it damps the higher Chebyshev modes more than the Crank–Nicolson scheme does.

We emphasize the fact that the matrix $\mathbf{E}$ does not possess the properties permitting us to conclude that $\rho(\mathbf{E})\le 1$ is sufficient for stability.[28,29] So $\mathbf{E}$ is not normal and when it is

diagonalizable (Crank–Nicolson scheme, for example) the dependence on Δt of the matrix of eigenvectors of $\mathbf{E}$ prevents us obtaining a criterion of algebraic stability[29] which would ensure the convergence of the scheme. However, numerical experiments conducted in Reference 21 in the case of the tau Chebyshev approximation (for which the same conclusions (i)–(iii) hold too) have shown that the Crank–Nicolson scheme as well as the second-order backward Euler scheme (for which $\mathbf{E}$ is not diagonalizable) are actually unconditionally stable.

8. NUMERICAL RESULTS FOR THE NAVIER–STOKES EQUATIONS

First the spatial accuracy of the method for solving the Navier–Stokes equations has been tested on the exact solution

$$\psi_{ex}^{(1)}=(1-x^2)^2(1-y^2)^2\,e^{x(y-1)}, \qquad \omega_{ex}^{(1)}=-\Delta\psi_{ex}^{(1)}. \tag{61}$$

which defines f in (1) and $g=h=0$ in (5). The steady solution is computed by means of the AB/2BE scheme ($\varepsilon=2$, $\theta_1=1$, $\theta_2=0$ in (8)) with $\mathbf{V}=\mathbf{0}$, $\omega=0$ as initial conditions and $\nu=1$. Table III gives the following errors: $E_1=E_\infty^\omega$, $E_2=E_2^\omega$ with E_∞^ω and E_2^ω defined in Section 6.2, $E_3=E_2^\omega$ obtained in Reference 20 with a tau collocation method. The comparison between E_2 and E_3 again shows the better accuracy of the present collocation method.

Then the accuracy in time has been checked on the unsteady solution

$$\psi_{ex}^{(2)}=\frac{2\pi-1+\sin(2\pi t)}{2\pi}\psi_{ex}^{(1)}, \qquad \omega_{ex}^{(2)}=-\Delta\psi_{ex}^{(2)}, \tag{62}$$

with $\psi_{ex}^{(1)}$ given in (61). This defines f in (1), $g=h=0$ in (5) and the initial condition (6), (7). The calculations have been done with $\nu=1$ and we have compared the error in time corresponding to various schemes of second-order accuracy:

A.	$\varepsilon=1$,	$\theta_1=1/2$,	$\theta_2=1/2$	(AB/CN scheme),
B.	$\varepsilon=2$,	$\theta_1=1$,	$\theta_2=0$	(AB/2BE scheme),
C.	$\varepsilon=1$,	$\theta_1=3/4$,	$\theta_2=0$,	
D.	$\varepsilon=3/2$,	$\theta_1=3/4$,	$\theta_2=1/4$.	

The degree of the polynomials is the same in both directions: $N=M=20$. This number is sufficient to represent correctly the spatial part of the solution (see Table III), so that the error which appears is actually the error in time. Figure 2 displays the error

$$E=\max_t\{\|\omega_{ex}^{(2)n}-\omega_{N,M}^n\|_2/\|\omega_{ex}^{(2)n}\|_2\}, \tag{63}$$

where $\omega_{ex}^{(2)n}$ and $\omega_{N,M}^n$ are the values of the exact solution and of the numerical solution respectively at $t=n\Delta t$; $\|\cdot\|_2$ is the discrete L_2 norm on the collocation points. The presence of three levels in time in the scheme necessitates a starting-up procedure with a modified scheme, which in the present case (Section 2) is first-order only. Hence the maximum in (63) is taken when the effect

Table III. Errors for the Navier–Stokes equations

$N=M$	E_1	E_2	E_3
10	2·21E−4	4·47E−5	1·37E−4
12	3·57E−6	5·38E−7	2·01E−6
16	2·52E−10	3·00E−11	1·29E−10
20	3·59E−12	7·74E−13	2·22E−12

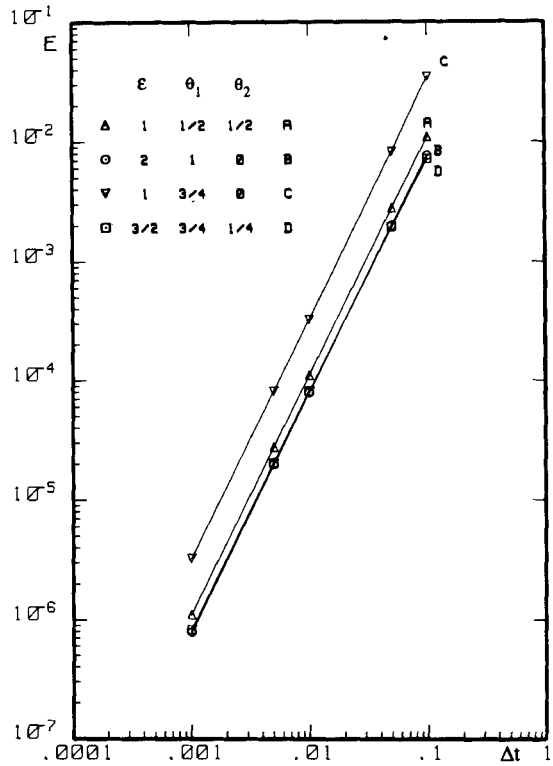

Figure 2. Error E is a function of Δt for various schemes

of the initialization has disappeared, that is when the periodicity of E is accurately established. It is seen in Figure 2 that the AB/2BE scheme is slightly more accurate than the AB/CN scheme, at least for the special solution considered here. The same conclusion was found in Reference 20.

Finally we have computed the steady flow in a square cavity $0 < X, Y < a$. The velocity is zero on three sides and is $u = -16\,u_r X^2(a^2 - X^2)/a^4$, $v = 0$ on the side $Y = a$. The Navier–Stokes equations are made dimensionless by using a, u_r and a/u_r as reference length, velocity and time respectively; Re is the corresponding Reynolds number. Then the change of variables $x = 2X - 1$, $y = 2Y - 1$ is done in order to express the Navier–Stokes equations in the domain $D: -1 < x, y < 1$. The resulting equations were solved with the AB/2BE scheme by using homogeneous initial conditions. The degree of the polynomials is the same in both directions ($N = M$). Table IV shows the maximum time step Δt allowable for stability. We may observe the good stability properties of the scheme: for instance, for $Re = 400$ the critical Δt varies approximately as $1/N$.

The steady solution is assumed to be reached when the normalized maximum residual on the vorticity is 10^{-6}. Table V gives some characteristic results: M_1 is the maximum value of ψ on collocation points, M_2 is the maximum value of ω on the upper side $y = 1$ calculated on collocation points and M_3 is the analogous maximum but calculated on 201 equispaced points. The coordinates of the points where the maxima are reached are given in parenthesis. The quantity M_3 provides a significant measure of the degree of convergence of the spatial approximation. So, for $Re = 100$, $N = 32$ is sufficient to represent correctly the solution within a relative change of 10^{-5}. On the other hand, in the case $Re = 400$, $N = 32$ is not sufficient to get an optimal representation of

Table IV. Critical time step Δt (with an error $\pm 10^{-3}$)

$N=M$	$Re=100$	$Re=400$
16	0·194	0·067
24	0·100	0·047
32	0·072	0·033

Table V. Results for the cavity flow

	$Re=100$			Re=400		
$N=M$	M_1	M_2	M_3	M_1	M_2	M_3
16	8·5159E−2 (0·40–0·78)	13·3687 (0·60)	13·4663 (0·62)	8·5378E−2 (0·40–0·60)	25·2329 (0·60)	25·4675 (0·62)
20	8·2695E−2 (0·42–0·73)	13·1780 (0·66)	13·4459 (0·62)	8·5213E−2 (0·43–0.58)	24·6693 (0·65)	24·9846 (0·63)
24	8·3315E−2 (0·37–0.75)	13·4227 (0·63)	13·4446 (0·62)	8·5716E−2 (0·43–0·63)	24·9344 (0·63)	24·9333 (0·63)
32	8·3402E−2 (0·40–0·74)	13·3422 (0·60)	13·4447 (0·62)	8·5480E−2 (0·40–0·60)	24·7845 (0·65)	24·9110 (0·63)

the solution. Figure 3 compares the values of M_3 given by various spectral methods and we refer to Reference 15 for analogous results obtained with finite difference methods.

Th CPU time on the CRAY 1S is $3{\cdot}36 \times 10^{-3}$ s/time step for $N=M=16$ and $1{\cdot}32 \times 10^{-2}$ s/time step for $N=M=32$.

9. DOUBLE-DIFFUSIVE CONVECTION

9.1. Formulation of the problem

Double-diffusive convection deals with the motion of a fluid resulting from the combined effet of gravitational acceleration and the diffusion of two components with different molecular diffusivities. As usual, we designate by T, temperature, the component with the higher diffusivity κ_T and by S, salinity, the other component with diffusivity κ_S.

In this section we are interested in the application of the collocation Chebyshev method to the calculation of the motion occurring when a fluid is salted and heated from below. This problem has already been studied numerically in References 30–35 by various methods, but none of these was able to give results for the case of small values of the ratio $\tau=\kappa_S/\kappa_T$ corresponding to actual values of salt and heat in water ($\tau \approx 10^{-2}$) because of the numerical difficulties associated with the complex structure of the salinity fields. Moreover, when τ is small the large disparity between the two time characteristic scales (thermal and solutal times) makes this a problem of the stiff type. The numerical results given below in the case where $\tau=0{\cdot}0125$ will show the ability of the Chebyshev method to compute such flow fields.

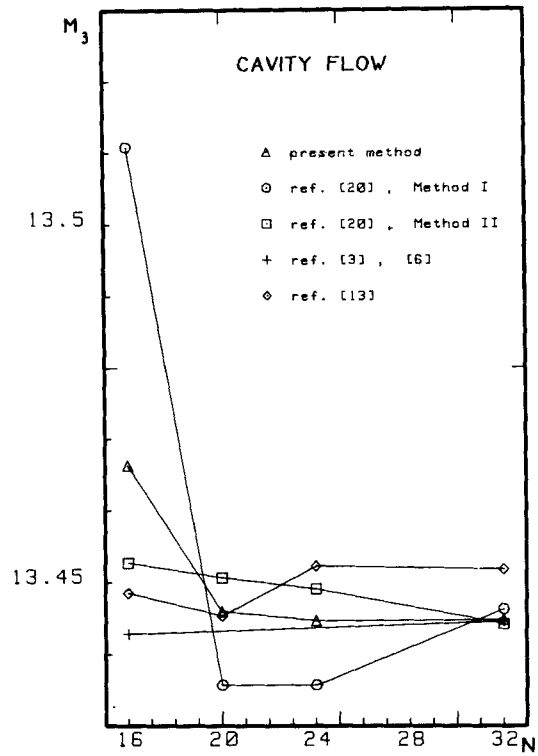

Figure 3. Maximum value of the vorticity $M_3 = \max \omega(x, y)$ on the moving boundary $y = 1$

In References 30, 31 and 33–35 the flow takes place in an infinite horizontal strip, the periodicity is assumed in the horizontal direction and the horizontal boundaries are assumed to be stress-free. Finite difference methods are used in References 31, 33–35 and a Fourier series method is considered in Reference 30. The case of a finite domain with no-slip boundary conditions was computed in Reference 32 using a first-order finite difference method.

Here we consider the case of a finite rectangular domain D: $0 < x < A$, $0 < y < 1$, the height H of the domain being taken as the characteristic length. In dimensionless variables the temperature T and salinity S are equal to one at the bottom, $y = 0$, and are zero at the top, $y = 1$. The vertical walls $x = 0$ and $x = A$ are such that $\partial T/\partial x = \partial S/\partial x = 0$. Finally, no-slip boundary conditions are considered for the velocity.

We are interested in the stability of the conductive solution $\mathbf{V}_0 = (u_0, v_0) = (0, 0)$, $T_0 = 1 - y$, $S_0 = 1 - y$; hence, by introducing the perturbation variables

$$\theta = T - (1 - y), \qquad \sigma = S - (1 - y) \tag{64}$$

and assuming the Boussinesq approximation to be valid, the equations of motion are written

$$\partial\theta/\partial t + \mathbf{V}\cdot\nabla\theta - v - \Delta\theta = 0, \tag{65}$$

$$\partial\sigma/\partial t + \mathbf{V}\cdot\nabla\sigma - v - \tau\Delta\sigma = 0, \tag{66}$$

$$\partial\omega/\partial t + \mathbf{V}\cdot\nabla\omega - Pr\,\Delta\omega = Pr(R_T\,\partial\theta/\partial x - R_S\,\partial\sigma/\partial x), \tag{67}$$

$$\Delta\psi + \omega = 0, \tag{68}$$

where Pr is the Prandtl number, R_T and R_S are the thermal and saline Rayleigh numbers respectively. The time has been normalized by using the thermal time H^2/κ_T as reference. The above equations are solved in the domain D with no-slip conditions $\psi = \partial\psi/\partial n = 0$ on the whole boundary and homogeneous boundary conditions for θ and σ, *i.e.* $\theta = \sigma = 0$ on $y = 0$ and $y = 1$, and $\partial\theta/\partial x = \partial\sigma/\partial x = 0$ on $x = 0$ and $x = A$.

At initial time the conductive solution is perturbed by considering the initial condition

$$\theta = \theta^\circ(x, y) = \cos(\pi x/A)\sin(\pi y), \qquad \sigma = 0, \qquad u = v = 0, \qquad \omega = 0. \tag{69}$$

The time discretization scheme makes use of the Adams–Bashforth second-order backward Euler scheme. Thus, at each time cycle, θ^{n+1} and σ^{n+1} are first calculated independently as the solution of Helmholtz equations obtained from (65) and (66) respectively. Then the resulting values are brought into the right-hand side of (67) and $(\omega^{n+1}, \psi^{n+1})$ is the solution of a Stokes-type problem. All these equations are solved by the collocation Chebyshev method described in the previous sections.

9.2. Numerical results

As found in References 30–35, different flow regimes exist according to the values of the physical parameters: steady or oscillatory (periodic or not) solutions with a possible hysteresis effect. Hence it is not our purpose here to make a detailed analysis of the problem, which would necessitate not only many more numerical experiments than we did but also a precise theoretical study. We only want to illustrate the ability of the method to solve a problem in a situation (small values of the diffusivity ratio) which has not yet been studied with any other numerical method.

In a first set of experiments we have considered the case already computed in Reference 32 with $A = 1$, $Pr = 1$, $\tau = 0{\cdot}1$, $R_S = 2000$ and various values of R_T. Our numerical results obtained with the initial condition (69) show the same behaviour as found in Reference 32: for small values of R_T the perturbation is damped out and the state is ultimately motionless; for large values of R_T we obtain a steady convective flow; between these values there exists a range of R_T for which the solution is periodic in time. Table VI give some results: $\psi_{\max}$ is the value of the streamfunction at the collocation point where its absolute value is maximum; N_T and N_S are respectively the thermal and saline Nusselt numbers averaged along the lower horizontal wall. In Table VI the columns (a) refer to our present results and (b) to the finite difference solution obtained in Reference 32. We observe some difference in the critical values of the thermal Rayleigh number R_T as well as in the values of $\psi_{\max}$, N_T and N_S. The error associated with the first-order finite difference approximation used in Reference 32 has the effect of increasing the critical value of R_T. Moreover, the difference in the sign of $\psi_{\max}$ means that the direction of rotation of the fluid is opposite. In fact, it is

Table VI. Results for $A = 1$, $Pr = 1$, $\tau = 0{\cdot}1$ and $R_S = 2000$: (a) present results; (b) results of Reference 32

	$\psi_{\max}$		N_T		N_S	
R_T	(a)	(b)	(a)	(b)	(a)	(b)
4800	0	0	1	1	1	1
4900	osc.	0	osc.	1	osc.	1
5000	−2·756	0	1·401	1	3·272	1
5200	−3·129	osc.	1·483	osc.	3·439	osc.
5450	−3·463	2·28	1·554	1·36	3·579	3·55
6000	−4·031	3·20	1·670	1·57	3·797	4·14

easy to verify on the steady equations of motion that steady convective solutions with both direct and indirect rotation are simultaneously possible.

For the periodic solution obtained for $R_T = 4900$ the period is found to be 0·545, with $-1{\cdot}681 \leq \psi_{max} \leq 1{\cdot}681$, $1{\cdot}002 \leq N_T \leq 1{\cdot}157$ and $1{\cdot}256 \leq N_S \leq 1{\cdot}625$. All the above calculations have been done with $N = M = 20$ and $\Delta t = 10^{-3}$.

In Reference 32 the authors reported that they always obtained the same final solution whatever the chosen initial condition. We have not studied the influence of the initial condition for $\tau = 0{\cdot}1$; on the other hand we did in the case $\tau = 0{\cdot}0125$ (not studied in Reference 32) and we find an important sensitivity of the solution to the initial condition $\theta^0(x, y)$. For example, with θ^0 given by (69) we obtain a periodic solution for $R_T = 4000$ (see Table VII), while by using the initial condition

$$\theta^0(x, y) = \cos \pi(x + \pi/10) \sin \pi(y + \pi/10) \tag{70}$$

we do not obtain such a periodic solution. More precisely, for $R_T \leq 4321$ the ultimate solution is the rest and for $R_T \geq 4322$ it is a steady convective state. Note that for these limiting values of R_T the equations have been integrated up to $t = 250$ (i.e. 3·125 characteristic solutal times). More calculations would be needed to determine the conditions of existence of oscillatory convection. Also a careful theoretical study would be necessary to clarify the question of the influence of initial conditions. At the moment we only want to point out that the initial condition (69) possesses the symmetry property $\phi(x, y) = -\phi(A - x, 1 - y)$ (where ϕ represents θ, σ, u or v), while the condition (70) does not. The above symmetry property induces an identical one for the solution at subsequent times and may have an influence on the behaviour of the solution.[33,34] One might think that such a periodic symmetrical solution is unstable to unsymmetrical perturbations; however, calculations have shown that the disturbances in the periodic regime created by a small random perturbation of the thermal field are damped out and the solution again becomes periodic.

The results presented in Table VII were obtained with the initial condition (69) and $A = 1$, $Pr = 1$, $\tau = 0{\cdot}0125$, $R_S = 2000$ and $N = M = 40$, $\Delta t = 5 \times 10^{-4}$. Figure 4 shows an example of the steady convective solution. In the case of the periodic solution ($R_T = 4000$) the period was found equal to 1·033 and $-1{\cdot}793 \leq \psi_{max} \leq 1{\cdot}793$, $1{\cdot}002 \leq N_T \leq 1{\cdot}194$, $2{\cdot}250 \leq N_S \leq 2{\cdot}999$. The graph of these quantities as a function of time is given in Figure 5. Figure 6, which shows the fields at various times (not equally spaced) during a period, illustrates the unsteady behaviour of the flow. The calculations have been pursued up to $t = 100$ in this latter case and up to $t = 250$ for $R_T = 3950$ and 4050.

From Table VII we notice a change in the direction of the steady flow for $R_T = 4400$. This also occurs for neighbouring values of R_T. We recall that steady solutions with rotation in both directions are possible.

Table VII. Results for $A = 1$, $Pr = 1$, $\tau = 0{\cdot}0125$ and $R_S = 2000$

R_T	ψ_{max}	N_T	N_S
3950	0	1	1
4000	osc.	osc.	osc.
4050	−2·502	1·359	6·303
4400	3·007	1·472	6·795
4600	−3·238	1·523	7·002
5000	−3·641	1·608	7·338

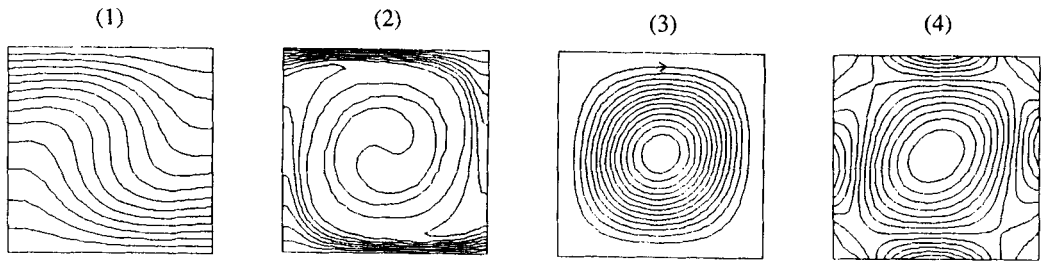

Figure 4. Contours of (1) temperature, (2) salinity, (3) streamfunction, (4) vorticity for $Pr=1$, $\tau=0{\cdot}0125$, $R_S=2000$, $R_T=5000$ (steady solution)

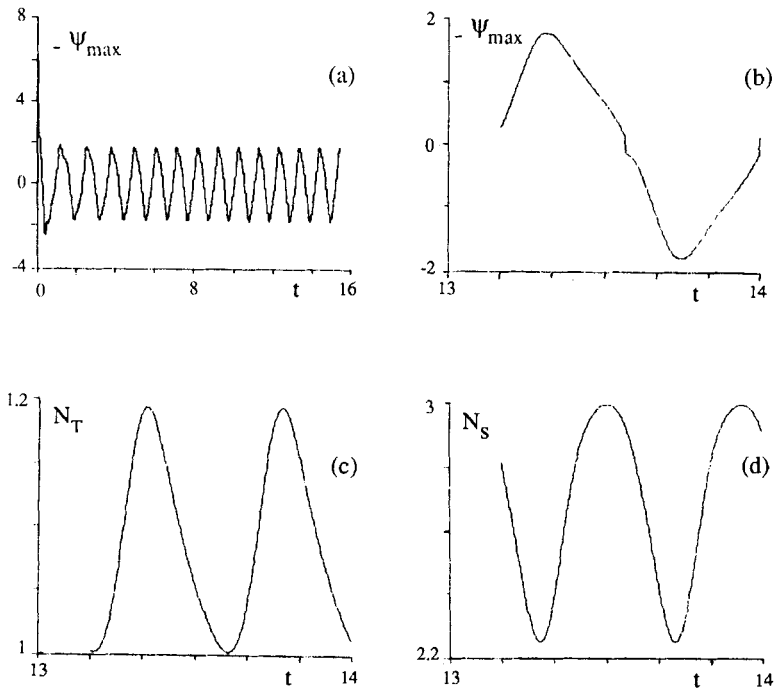

Figure 5. Evolution in time of (a), (b) maximum streamfunction, (c) thermal Nusselt number, (d) saline Nusselt number for $Pr=1$, $\tau=0{\cdot}0125$, $R_S=2000$, $R_T=4000$ (periodic solution)

Some calculations have also been done with a realistic value of the Prandtl number for salted water, i.e. $Pr=7$. We present here some results obtained with the initial condition (69) and $A=2$, $\tau=0{\cdot}0125$, $R_S=10^4$ and two values of R_T. These calculations were carried out with $N=60$, $M=40$ and $\Delta t=5\times10^{-4}$. For $R_T=2\times10^4$ the ultimate solution is the steady convective flow illustrated in Figure 7. In this case it is clear that the salinity is nearly constant (equal to 1/2) everywhere except in the neighbourhood of the walls, in particular near the horizontal walls where it exhibits a boundary layer behaviour. Finally, Figure 8 presents some typical fields at different times for $R_T=1{\cdot}2\times10^4$. These fields show how complex the salinity structure can become when the

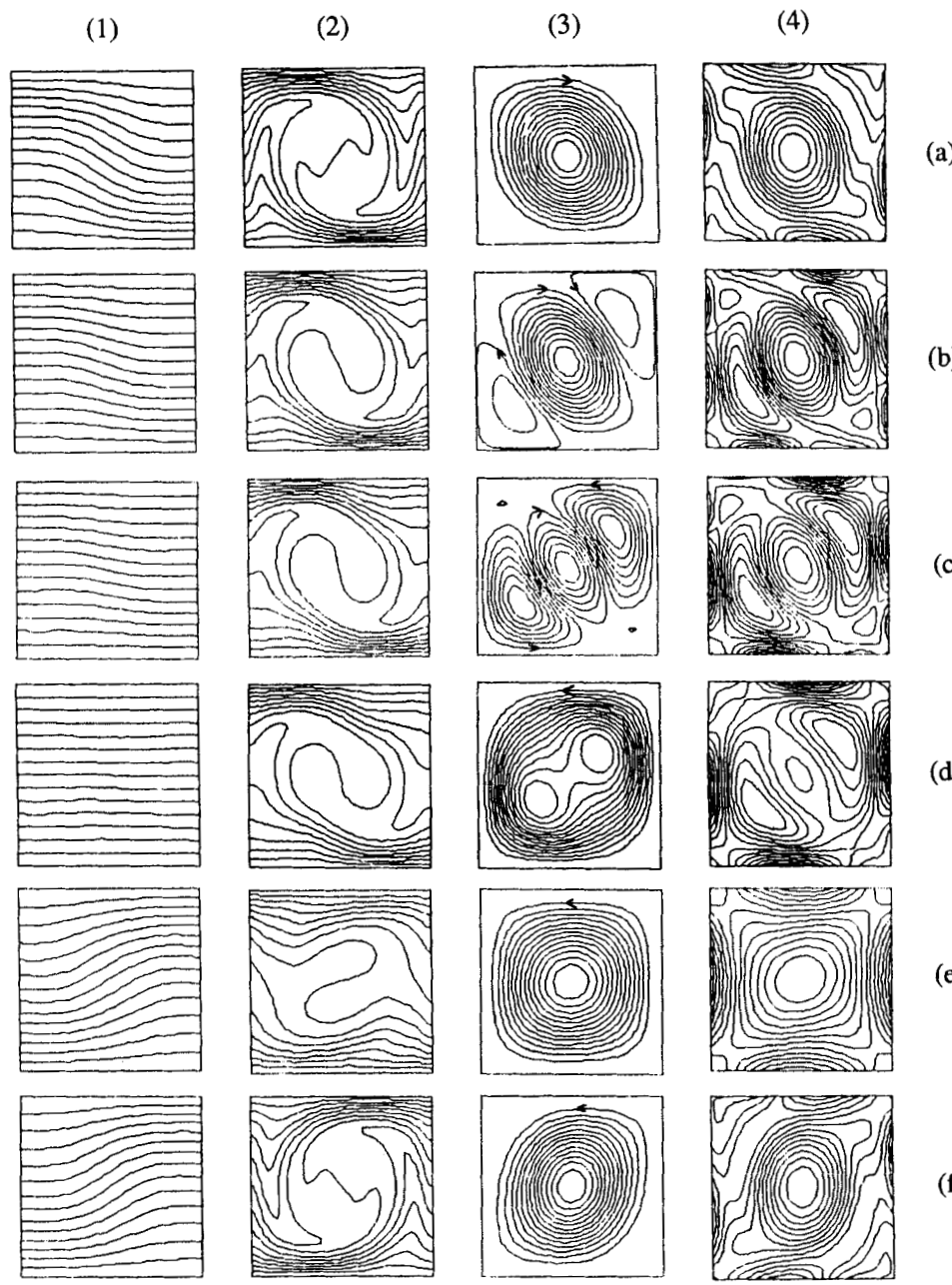

Figure 6. Instantaneous contours of (1) temperature, (2) salinity, (3) streamfunction, (4) vorticity for $Pr = 1$, $\tau = 0{\cdot}0125$, $R_S = 2000$, $R_T = 4000$ at times (a) 13·52, (b) 13·64, (c) 13·68, (d) 13·72, (e) 13·84, (f) 14·04 (periodic solution)

diffusivity ratio is small. This case has not been computed for a time long enough to decide about the nature of the ultimate state.

All these calculations show how careful one must be when using a direct simulation for studying multiple solutions. Very often a large integration time is needed to ensure that a periodic or steady

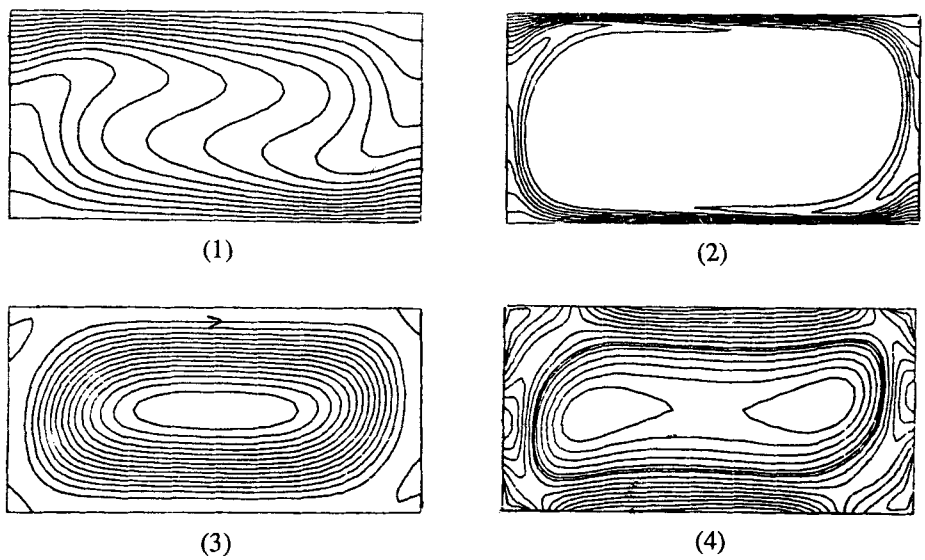

Figure 7. Contours of (1) temperature, (2) salinity, (3) streamfunction, (4) vorticity for $Pr=7$, $\tau=0{\cdot}0125$, $R_S=10^4$, $R_T=2\times10^4$ (steady solution)

state, up to the machine accuracy, is actually reached; also the level of accuracy of the calculations can have an effect on the behaviour of the solution. In these respects an analytical study based on the theory of stability and bifurcation is a valuable complement to a direct simulation.

10. CONCLUSIONS

A Chebyshev collocation method has been developed for solving the Navier–Stokes equations within the vorticity–streamfunction formulation. The efficiency of the method is mainly due to the influence matrix technique used to prescribe the boundary conditions correctly. Then the computational effort reduces to matrix products which can be performed efficiently on a vector computer. The evaluation of the non-linear terms can be done either by matrix products or by the pseudospectral technique using the fast Fourier transform algorithm. For the time discretization it has been shown that the finite difference Adams–Bashforth/second-order backward Euler scheme possesses good properties of stability and accuracy. The accuracy of the spatial Chebyshev polynomial approximation has been examined on test cases. Finally the capability of the method to solve a more realistic problem has been proven by computing a double-diffusive convective flow in a rather delicate situation because of the small value of the diffusivity ratio.

The main advantage of the present collocation method over the tau collocation method proposed in Reference 20 lies in the fact that ψ and ω are approximated with polynomials of the same degree while in the tau collocation case ψ is approximated with higher-degree polynomials than ω. This produces two different sets of collocation points for ψ and ω and then necessitates a special numerical treatment for evaluating the normal derivative of ψ at the boundary and for computing the non-linear terms by FFT. The present method is free of such difficulties. Moreover, the collocation influence matrix is better conditioned than the tau collocation one. Finally, as recognized in several circumstances, the collocation method also possesses other advantages over the tau method: better accuracy and stability, easier solution of variable coefficients equations.

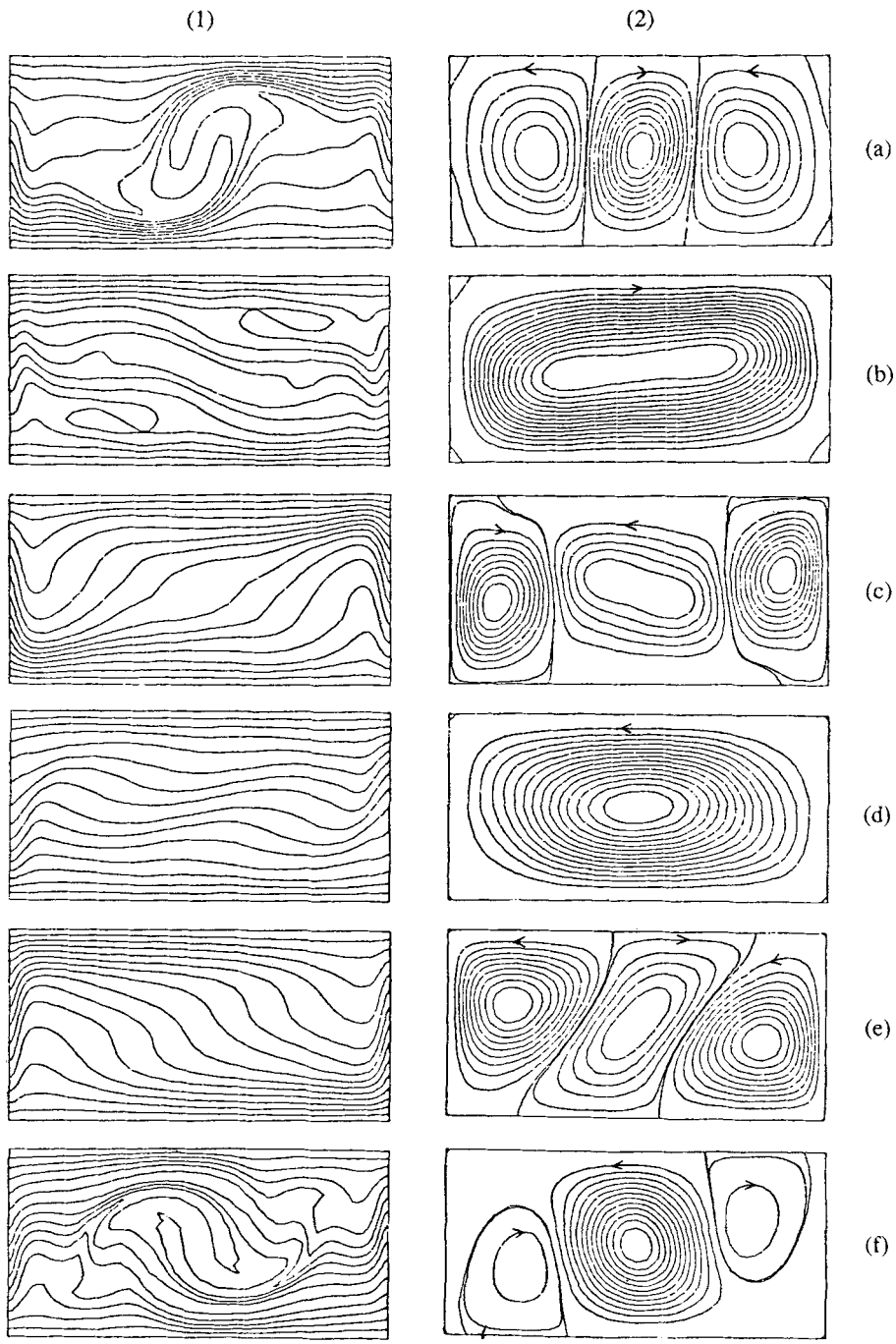

Figure 8. Instantaneous contours of (1) salinity, (2) streamfunction for $Pr = 7$, $\tau = 0{\cdot}0125$, $R_S = 10^4$, $R_T = 1{\cdot}2 \times 10^4$ at times (a) 0·6, (b) 0·8, (c) 0·92, (d) 1·0, (e) 1·08, (f) 1·40 (unsteady solution)

ACKNOWLEDGEMENT

The authors are grateful to B. Lhomme for his assistance. The computations have been supported by the 'Centre de Calcul Vectoriel pour la Recherche'.

APPENDIX: COEFFICIENTS OF DERIVATIVE EXPANSIONS (EQUATION (19))

First-order derivative

$$d_N^{(1)}(k,j)=\frac{\bar{c}_k}{\bar{c}_j}\frac{(-1)^{k+j}}{x_k-x_j}, \quad 0\le k,j\le N, \quad k\neq j,$$

$$d_N^{(1)}(k,k)=-\frac{x_k}{2(1-x_k^2)}, \quad 1\le k\le N-1,$$

$$d_N^{(1)}(0,0)=-d_N^{(1)}(N,N)=\frac{2N^2+1}{6},$$

where $x_k=\cos(k\pi/N)$; $\bar{c}_0=\bar{c}_N=2$, $\bar{c}_k=1$, $1\le k\le N-1$.

Second-order derivative

$$d_N^{(2)}(k,j)=\frac{(-1)^{k+j+1}}{\bar{c}_j}\left(\frac{2-x_kx_j-x_k^2}{(1-x_k^2)(x_k-x_j)^2}\right), \quad 1\le k\le N-1, \quad k\neq j, \quad 0\le j\le N,$$

$$d_N^{(2)}(k,k)=-\frac{(N^2-1)(1-x_k^2)+3}{3(1-x_k^2)^2}, \quad 1\le k\le N-1,$$

$$d_N^{(2)}(0,j)=\frac{2}{3}\frac{(-1)^j}{\bar{c}_j}\frac{(2N^2+1)(1-x_j)-6}{(1-x_j)^2}, \quad 1\le j\le N,$$

$$d_N^{(2)}(N,j)=\frac{2}{3}\frac{(-1)^{j+N}}{\bar{c}_j}\frac{(2N^2+1)(1+x_j)-6}{(1+x_j)^2}, \quad 0\le j\le N-1,$$

$$d_N^{(2)}(0,0)=d_N^{(2)}(N,N)=\frac{N^4-1}{15}.$$

REFERENCES

1. S. A. Orszag and L. C. Kells, 'Transition to turbulence in plane Poiseuille and plane Couette flow', *J. Fluid Mech.*, **96**, 159–205 (1980).
2. P. Moin and J. Kim, 'On the numerical solution of time-dependent viscous incompressible fluid flows involving solid boundaries', *J. Comput. Phys.*, **35**, 381–392 (1980).
3. L. Kleiser and U. Schumann, 'Treatment of incompressibility and boundary conditions in 3-D numerical spectral simulations of plane channel flows', in E. H. Hirschel (ed.), *Proc. Third GAMM Conf. on Numerical Methods in Fluid Mechanics*, Vieweg, Braunschweig, 1980, pp. 165–173.
4. Y. Morchoisne, 'Résolution des équations de Navier–Stokes par une méthode spectrale de sous-domaines', *3ème Conf. Int. sur les Méthodes Numériques de l'Ingénieur GAMNI*, Paris, 14–16 March 1983.
5. J. Ouazzani and R. Peyret, 'A pseudo-spectral solution of binary gas mixture flows', in M. Pandolfi and R. Piva (eds), *Proc. Fifth GAMM Conf. on Numerical Methods in Fluid Mechanics*, Vieweg, Braunschweig, 1984, pp. 275–282.
6. J. Ouazzani, R. Peyret and A. Zakaria, 'Stability of collocation–Chebyshev schemes with application to the Navier–Stokes equations', in D. Rues and W. Kordulla (eds), *Proc. Sixth GAMM Conf. on Numerical Methods in Fluid Mechanics*, Vieweg, Braunschweig, 1986, pp. 287–294.
7. P. Haldenwang, 'Résolution tridimensionnelle des équations de Navier–Stokes par méthodes spectrales Tchebycheff: application à la convection naturelle', *Thèse Doctorat d'Etat*, Université de Provence, Marseille, 1984.

8. P. Le Quéré and T. Alziary de Roquefort, 'Computation of natural convection in two-dimensional cavities with Chebyshev polynomials', *J. Comput. Phys.*, **57,** 210–228 (1985).
9. M. R. Malik, T. A. Zang and M. Y. Hussaini, 'A spectral collocation method for the Navier–Stokes equations', *J. Comput. Phys.*, **61,** 64–88 (1985).
10. F. Montigny-Rannou and Y. Morchoisne, 'A spectral method with staggered grid for incompressible Navier–Stokes equations', *Int. j. numer. methods fluids*, **7,** 175–189 (1987).
11. H. C. Ku, T. D. Taylor and R. S. Hirsh, 'Pseudospectral methods for solution of the incompressible Navier–Stokes equations', *Comput. Fluids*, **15,** 195–214 (1987).
12. B. Bondet de la Bernardie, 'Contribution à la modélisation et à la simulation numérique du comportement dynamique et thermique des fluides visqueux par les méthodes spectrales', *Thèse Doctorat 3ème cycle*, Mécanique des Fluides, Université Aix-Marseille III, 1980.
13. F. Elie, A. Chikhaoui, A. Randriamampianina, P. Bontoux and B. Roux, 'Spectral approximation for Boussinesq double-diffusion', in M. Pandolfi and R. Piva (eds), *Proc. Fifth GAMM Conf. on Numerical Methods in Fluid Mechanics*, Vieweg, Braunschweig, 1984, pp. 57–64.
14. J. C. Wu and M. M. Wahbah, 'Numerical solution of viscous flow equations using integral representations', *Proc. Fifth Int. Conf. on Numerical Methods in Fluid Dynamics*; *Lecture Notes in Physics*, **59,** 448–453 (1976).
15. R. Peyret and T. D. Taylor, *Computational Methods for Fluid Flow*, Springer Verlag, 1983.
16. R. Glowinski and O. Pironneau, 'Numerical methods for the biharmonic equation and for the two dimensional Stokes problem', *SIAM Rev.*, **12,** 167–212 (1979).
17. S. C. R. Dennis and L. Quartapelle, 'Direct solution of the vorticity–stream function ordinary differential equations by a Chebyshev approximation', *J. Comput. Phys.*, **52,** 448–463 (1983).
18. S. C. R. Dennis and L. Quartapelle, 'Spectral algorithms for vector elliptic equations in a spherical gap', *J. Comput. Phys.*, **61,** 218–241 (1985).
19. L. Tuckerman, 'Formation of Taylor vortices in spherical Couette flow', *Ph.D. Thesis*, MIT, Cambridge, 1983.
20. J. M. Vanel, R. Peyret and P. Bontoux, 'A pseudo-spectral solution of vorticity–stream function equations using the influence matrix technique', in K. W. Morton and M. J. Baines (eds), *Numerical Methods for Fluids Dynamics II*, Clarendon Press, Oxford, 1986, pp. 463–475.
21. U. Ehrenstein, 'Méthodes spectrales de résolution des équations de Stokes et de Navier–Stokes. Application à des écoulements de convection double-diffusive', *Thèse Doctorat*, Mathématiques appliquées, Université de Nice, 1986.
22. U. Ehrenstein and R. Peyret, 'A collocation Chebyshev method for solving Stokes-type equations', *Sixth Int. Symp. on Finite Element Methods in Flow Problems*, Antibes, 16–20 June, 1986.
23. D. B. Haidvogel and T. Zang, 'The accurate solution of Poisson's equation by expansion in Chebyshev polynomials', *J. Comput. Phys.*, **30,** 167–180 (1979).
24. D. Gottlieb and L. Lustman, 'The spectrum of the Chebyshev collocation operator for the heat equation', *SIAM J. Numer. Anal.*, **20,** 903–921 (1983).
25. P. Haldenwang, G. Labrosse, S. Abboudi and M. Deville, 'Chebyshev 3-D spectral and 2-D pseudospectral solvers for the Helmholtz equation', *J. Comput. Phys.*, **55,** 115–128 (1984).
26. C. Canuto and A. Quarteroni, 'Preconditioned minimal residual methods for Chebyshev spectral calculations', *J. Comput. Phys.*, **60,** 315–357 (1985).
27. Y. Demay, J. M. Lacroix, R. Peyret and J. M. Vanel, 'Numerical experiments on stratified fluid subject to heating', *Third Int. Symp. on Stratified Flow*, Pasadena, 3–5 February, 1987.
28. A. R. Gourlay and D. F. Griffiths, *The Finite Difference Method in Partial Differential Equations*, Wiley, 1980.
29. S. A. Orszag and D. Gottlieb, *Numerical Analysis of Spectral Methods*; *Theory and Applications*, CBMS Regional Conference Series in Applied Mathematics, SIAM, 1977.
30. G. Veronis, 'Effect of a stabilizing gradient of solute on thermal convection', *J. Fluid Mech.*, **34,** 315–336 (1968).
31. H. E. Huppert and D. R. Moore, 'Nonlinear double-diffusive convection', *J. Fluid Mech.*, **78,** 851–854 (1976).
32. S. M. Chang, S. A. Korpela and Y. Lee, 'Double-diffusive convection in the diffusive regime', *Appl. Sci. Res.*, **39,** 301–319 (1982).
33. E. Knobloch, D. R. Moore, J. Toomre and N. O. Weiss, 'Transitions to chaos in two-dimensional double-diffusive convection', *J. Fluid Mech.*, **166,** 409–448 (1986).
34. E. Knobloch, A. E. Deane, J. Toomre and D. R. Moore, 'Double diffusive waves', *Contemp. Math.*, **56,** 203–216 (1986).
35. A. E. Deane, E. Knobloch and J. Toomre, 'Traveling waves and chaos in thermolutal convection', *Phys Rev. A*, **36,** 2862–2869 (1987).